

Two dimensional finite element modeling of Tabriz metro underground station L2-S17 in the marly layers

Hadiseh Mansouri* and Ebrahim Asghari-Kalajahi^a

Department of Earth Sciences, University of Tabriz, Tabriz, Iran

(Received July 23, 2019, Revised October 25, 2019, Accepted November 8, 2019)

Abstract. Deep excavations for development of subway systems in metropolitan regions surrounded by adjacent buildings is an important geotechnical problem, especially in Tabriz city, where is mostly composed of young alluvial soils and weak marly layers. This study analyzes the wall displacement and ground surface settlement due to deep excavation in the Tabriz marls using two dimensional finite element method. The excavation of the station L2-S17 was selected as a case study for the modelling. The excavation is supported by the concrete diaphragm wall and one row of steel struts. The analyses investigate the effects of wall stiffness and excavation width on the excavation-induced deformations. The geotechnical parameters were selected based on the results of field and laboratory tests. The results indicate that the wall deflection and ground surface settlement increase with increasing excavation depth and width. The change in maximum wall deflection and ground settlement with considerable increase in wall stiffness is marginal, however the lower wall stiffness produces the larger wall and ground displacements. The maximum wall deflections induced by the excavation with a width of 8.2 m are 102.3, 69.4 and 44.3 mm, respectively for flexible, medium and stiff walls. The ratio of maximum ground settlement to maximum lateral wall deflection approaches to 1 with increasing wall stiffness. It was found that the wall stiffness affects the settlement influence zone. An increase in the wall stiffness results in a decrease in the settlements, an extension in the settlement influence zones and occurrence of the maximum settlements at a larger distance from the wall. The maximum of settlement for the excavation with a width of 14.7 m occurred at 6.1, 9.1 and 24.2 m away from the wall, respectively, for flexible, medium and stiff walls.

Keywords: deep excavation; finite element method; Tabriz Metro Line 2; Marl

1. Introduction

Deep excavations in urban areas are of complex soil-structure interaction problems (Dong *et al.* 2014). They can have undesirable influences on adjacent buildings and other public utilities (Do *et al.* 2014, Fonte 2010, Nawel and Salah 2015, Zheng *et al.* 2017), especially in soft ground (Hesami *et al.* 2013). The horizontal stress relaxation by the excavation induces large deflection of the retaining wall accompanied by vertical deformation (settlement) for the soil around the excavation (Ahmed and Fayed 2015). To avoid damage to adjacent structures or existing buildings, analysis of deep excavation and prediction of lateral wall deflections and ground surface settlements is required, usually before the start of the design process (Hsieh and Ou 1998). Deep excavations cannot be analyzed using simple analytical methods due to their complex nature (Hung *et al.* 2014). Instead, the finite element method (FEM) and the empirical method are two common ways for analyzing deep excavations and predicting ground surface settlement. Nowadays, the FEM has become the prevalent technique used for analyzing excavation behavior. This method allows

applying various constitutive models for soil profile from a simple elastic model to mathematically complex non-linear elasto-plastic models. The effects of many factors on excavation behavior can be straightforwardly investigated by FEM. Studies by many researchers (e.g., Hsieh *et al.* 2003, Hsiung and Dao 2015, Ng *et al.* 2004, Yeow *et al.* 2006) show that FEM can predict wall deflection with good accuracy.

Deep excavations for development of rapid transit underground railways are of important geotechnical problems in Tabriz city, one of the major cities in northwest of Iran. In order to decrease the traffic problems of Tabriz, four lines urban railways are considered. The Tabriz Metro Line 2 (TML2) with an approximate length of 22 km and about 20 underground stations passes through the densely populated area of the city. This line will connect the western part of the city (Qaramalek region) to the eastern part of Tabriz at Basij Square (Fig. 1). Ground conditions at the each station of TML2 were investigated by at least two boreholes and sophisticated sampling to minimize the disturbance of the recovered cores. The entire route will be situated underground where the route is mostly covered by soft rocks (marlstone, claystone and siltstone layers) in the eastern parts. Soft rocks are critical geomaterials, since they present several types of problems. They may present undesirable behaviors, such as low strength, disaggregation, crumbling, high plasticity, slaking, fast weathering, and many other characteristics (Kanji 2014). They can produce significant plastic deformation under engineering forces (He

*Corresponding author, Ph.D.
E-mail: h.mansouri@tabrizu.ac.ir

^aAssociate Professor
E-mail: e-asghari@tabrizu.ac.ir

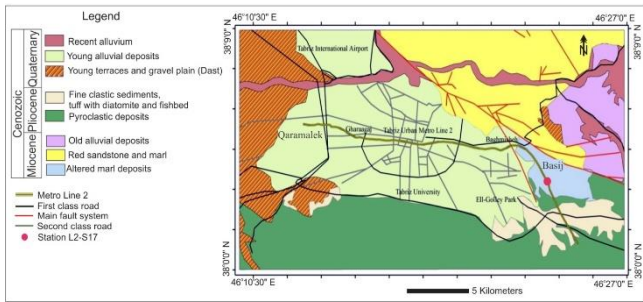


Fig. 1 Geological map of Tabriz city (Firuzi *et al.* 2019) and the location of station L2-S17



Fig. 2 Cracking and collapsing in the one of Tabriz Metro Line 2 stations

2014). Tabriz marls are classified into yellow, green and gray marls, based on their colors. Previous studies (e.g. Hooshmand *et al.* 2012) show that the yellow marls are stiff while green and gray marls are very stiff to hard. Major clay minerals of Tabriz marls are Illite, Kaolinite, Montmorillonite and Chloride. Based on Jalali-Milani *et al.* (2017) work, the uniaxial compressive strength of yellow, green and gray marls ranges from 100 to 250, 300 to 480 and 500 to more than 2000 kPa, respectively, which fall at the lowest limit of strength range proposed by ISRM (1981) for soft rocks (0.25 to 25 MPa). Hooshmand *et al.* (2012) findings show that the elastic modulus of yellow, green and gray marls is in the range of 10-12.5, 10-17.5 and 20 to more than 50 MPa, respectively. Tabriz marls, especially yellow marls, have a high potential for cracking, settlement and expansion due to its susceptibility to weathering processes (Jalali-Milani *et al.* 2017, Asghari Kaljahi *et al.* 2019). Fig. 2 shows cracking and collapse produced in one of the Tabriz Metro stations following tunneling and intensive rainfall in winter 2019. Deep excavations for development of metro tunnels and stations in these weak layers can carry major risks to nearby residential and commercial structures. Therefore, it is important to analyze excavation-induced deformations in these strata.

Although, excavation is a three-dimensional problem, the 3D analysis is much more time-consuming to perform and requires more memory than the 2D analysis (Sabzi and Fakher 2015). Ghahreman (2004) showed that the differences between the results of 3D and 2D models are negligible. This paper aims to present a two-dimensional finite element study of a deep excavation in Tabriz marly layers. Station L2-S17 in Narmak area (southern

Baghmisheh; Fig. 1) is chosen as the case study and the FEM code, PLAXIS is selected as the numerical analysis tool. The station L2-S17 is approximately rectangular in shape with widths of 16.4 m and 29.4 m, and a length of 150 m (Fig. 3(a)). Different cross sections of the station are shown in Fig. 3(b). The excavations in marly layers will be supported by the concrete diaphragm walls with one row of steel struts (Fig. 3(c)). Due to high stiffness, high strength, impermeability, etc, the diaphragm walls are the best retaining structures for deep excavations in soft ground (Wang *et al.* 2012). The displacements observations during construction process showed that the maximum ground settlement is more than 10 mm for the excavations supported by flexible walls. This is a large deformation for the densely populated area. Therefore, it is necessary to select the suitable stiffness for the concrete diaphragm walls. This study investigates the effects of wall stiffness and excavation width on the wall deflections and ground settlements in marly layers.

2. Geological setting

Tabriz city is located in Alborz-Azarbayjan geological zone (Nabavi 1976). Oun-Ebne Ali Mountains with E-W trend in north and Sahand volcano with low heights in south surround this city. General slope of the plain and general drainage of surface and sub-ground water is toward the west (Asghari-Kaljahi *et al.* 2015). The most important structural feature in Tabriz is the Tabriz North fault with the NW-SE trend which separates Tabriz plain from North Mountains. Many minor faults are also located in the southern parts of the city (Edalat *et al.* 2010).

The geological map of the city is shown in the Fig. 1. Tabriz plain is composed of young and unconsolidated deposits that are mostly formed from river and glacial sediments, with different textures and a variety of gradings (Mohammadi *et al.* 2015). These deposits are belong to Cenozoic and Quaternary (Firuzi *et al.* 2019). There is no sign of Pre-Miocene sediments. The oldest unit in Tabriz is the Upper Red formation which is mostly composed of layered sedimentary soft rocks (sandstone, mudstone, marl and thin layers of gypsum). This unit deposited in an upper Miocene to Pliocene basin during a time of intense tectonic and volcanism (Barzegari *et al.* 2018).

This formation is covered by Baghmisheh formation comprising of shale-marl units with the age of Miocene and Pliocene (Jalali-Milani *et al.* 2017). Generally, Tabriz marls with the colors of yellow, green and gray/black have the most outcrops in the Baghmisheh area. In most parts of the city, Baghmisheh formation is overlain by Pliocene units, including sediments with fish-fossils, marl, lapilli and diatomite. In fact, Tabriz city is mostly covered by recent alluvial sediments overlying the bedrock which is a complex of conglomerate, clay stone, sandstone and marl stone.

TML2 is located south of Oun-Ebne Ali mountains and passes through red clastic continental sediments (Upper Red formation) and Quaternary alluvial sediments (Nikvar Hassani *et al.* 2016). The bedrock has a shallow depth in the station L2-S17 so that marlstone and siltstone are seen at

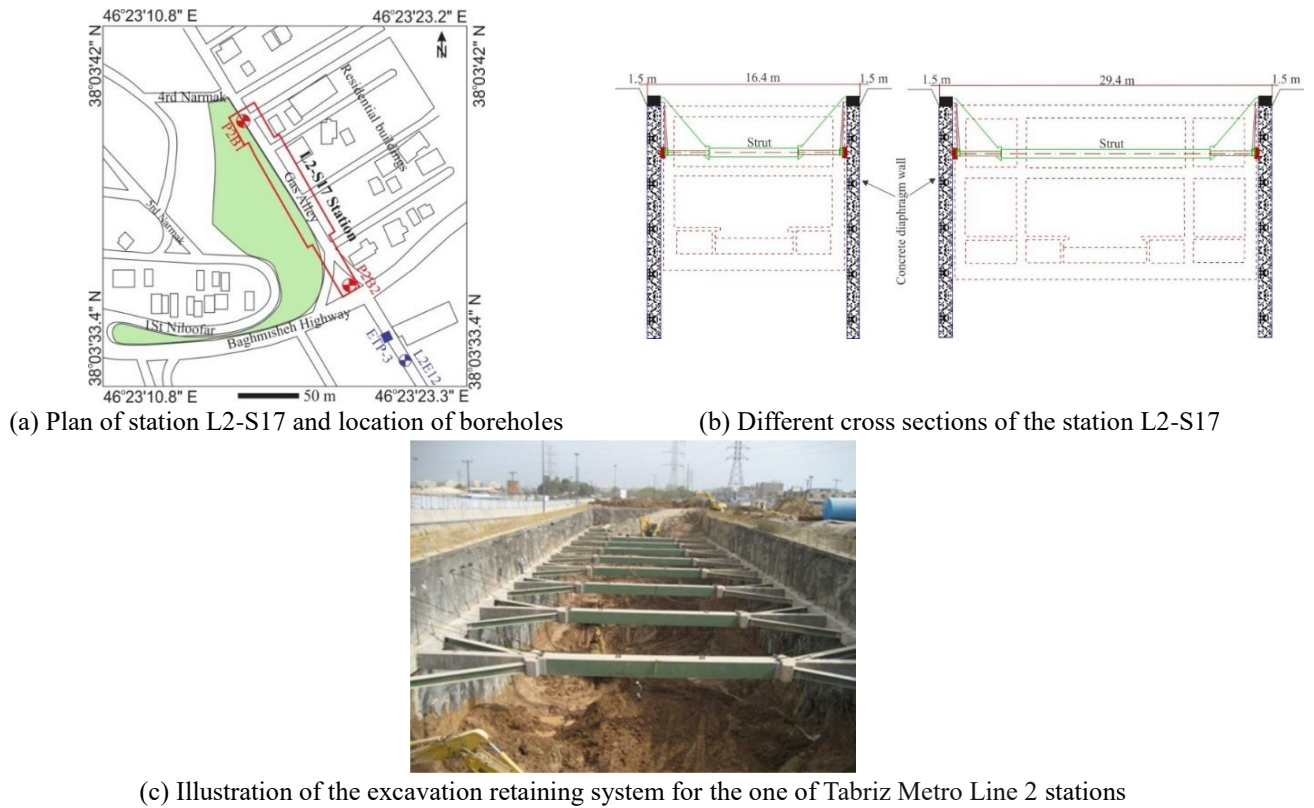


Fig. 3 A plan view and different cross sections of the station

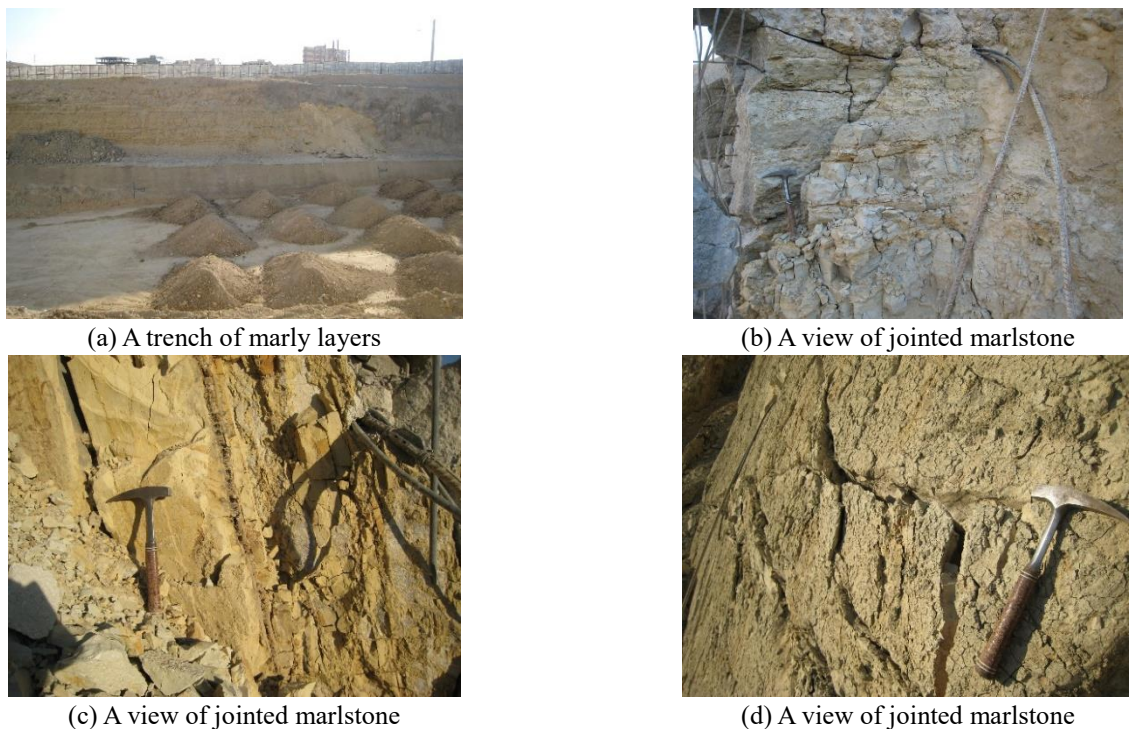


Fig. 4 A close-up view of marly layers in the station

the ground surface. Shallow marls are yellow to light-green while deeper marls are gray. Generally, stiffness of these marly layers increases with the depth. Fig. 4(a) shows a trench of the marly layers in this station. The marly layers at this site have a blocky to weathered appearance with macro and micro fractures (Fig. 4(b)-(d)).

3. Geotechnical condition of the study area

The station L2-S17 is located in a residential area of Tabriz city and is bounded by the intersection of Gas Alley and Pasdaran highway. The geology of the site was determined through three boreholes, L2E12, P2B1 and

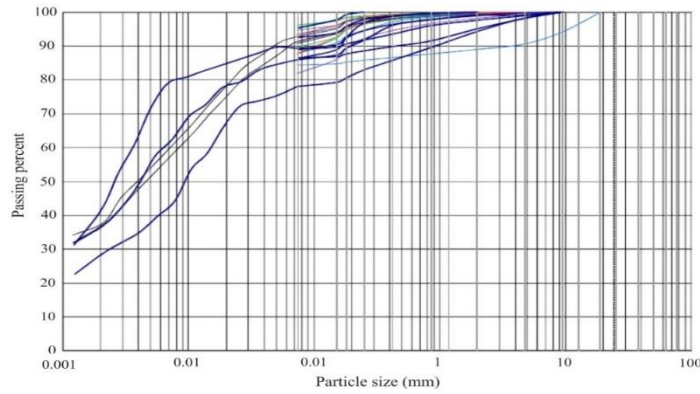


Fig. 5 Grain size distribution curves of the marly soils

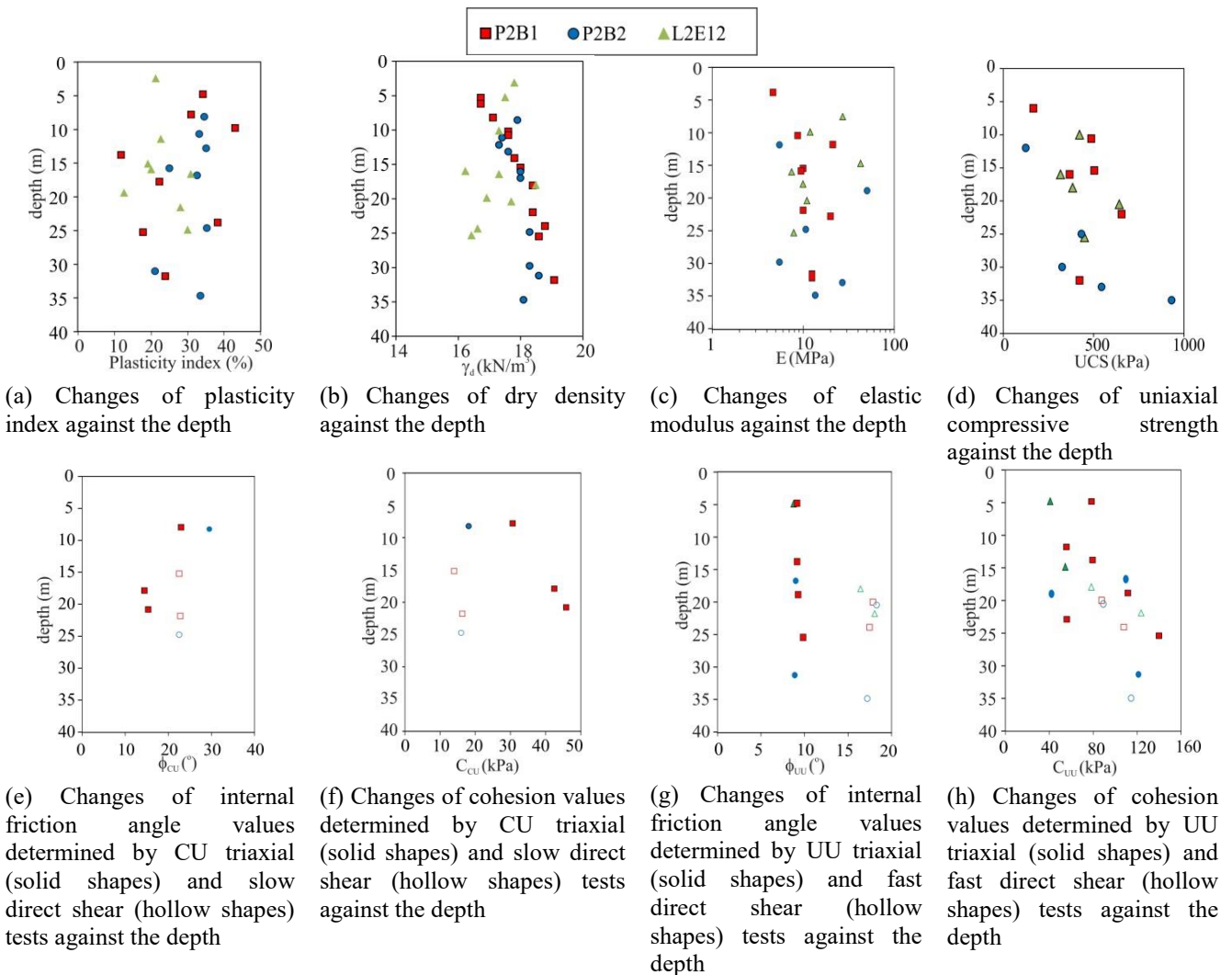
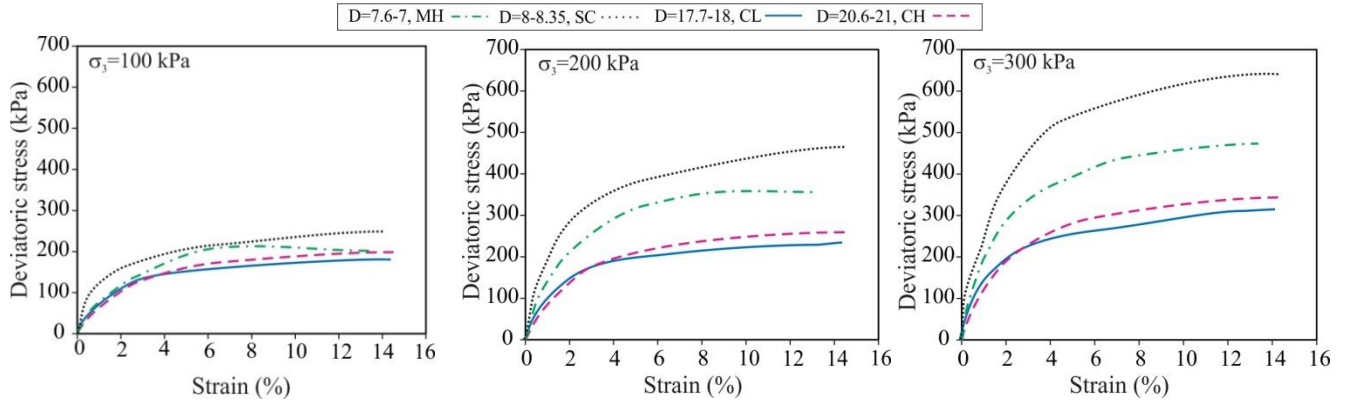


Fig. 6 Soil properties from the results of in-situ and laboratory tests

P2B2 with a depth of 30-35 m, and one test pit, ETP-3 with a depth of 5 m (Fig. 3(a)), with field tests and laboratory tests. Menard pressuremeter tests (PMT) and in-situ permeability tests were performed to determine the modulus of deformability and permeability of layers. For laboratory tests, classification tests, uniaxial compression tests, triaxial UU and CU tests and direct shear tests were conducted.

Groundwater depth ranges from 6.8 to 11 m during

various seasons. Groundwater is not under pressure based on observations during boreholes drillings (P. O. Rahvar Consulting Engineers 2008). The subsurface layers can be roughly divided into (1) man-made soils and coarse-grained alluvial sediments at a depth of 0-3 m, (2) weak marlstone with intercalations of claystone, siltstone and conglomerate at a depth of 3 to 8 m, (3) marly layers with thin interlayers of siltstone at a depth of 8 to 20 m and then (4) hard



(a) Stress-strain curves under confining pressure of 100 kPa

(b) Stress-strain curves under confining pressure of 200 kPa

(c) Stress-strain curves under confining pressure of 300 kPa

Fig. 7 Some deviatoric stress-strain curves of marlstone samples from different depths obtained in CU triaxial tests (D in the legend points to the sample depth)

marlstone layers with thin weak sandstone layers at below depth of 20 m. Based on the grain size distribution curves (Fig. 5) and plasticity index (Fig. 6(a)), siltstone, claystone and marlstone in deeper levels can be classified as low-and high-plasticity clay and silt with classes of CL, CH, ML and MH according to USCS. The soil properties from the results of in situ and laboratory tests are shown in Fig. 6.

The modulus of deformation values, determined by PMT, range from 20 to 51 MPa. These values are in concordance with those documented for the silty clay soils by Cheshomi and Ghodrati (2015). The uniaxial compressive strength (UCS) of the studied samples ranges from 125 to 932 kPa, and most samples have the UCS value lower than 500 kPa (Fig. 6(d)). The UCS value of 500 kPa was considered as the lower limit of soft rock strength by Dobereiner (1984). Therefore, the UCS values suggest that marlstone samples behave more like soil than rock.

The results of triaxial tests performed on marlstone samples indicated non-linear failure behavior. Some stress-strain curves of marlstone samples obtained in CU triaxial tests under confining pressures of 100, 200, 300 kPa are shown in Fig. 7. The stress-strain behavior of the samples exhibit obvious two stages during loading. Stage I: elastic deformation in which the strain grows linearly with increasing stress and the axial deviatoric stress-strain curve is almost a straight line. Stage II: plastic deformation in which the stress-strain curve gradually deviates from the straight line and continues with a positive slope. There is no clear peak in deviatoric stress for all specimens until axial strain of 14%. Ghazvinian *et al.* (2008) believes that this behavior is due to high cohesion of marlstone. The large percent of clay in the samples (Fig. 5) could be resulted in ductile behavior of them during uniaxial, triaxial and direct shear tests. Georgiannou *et al.* (1990) and Tenando (2004) believe that a large percentage of clay can postpone the axial strain at which peak shear strength occurs and subsequently lead to more ductility of the samples.

4. Finite element modeling

The excavation of the station L2-S17 was modeled

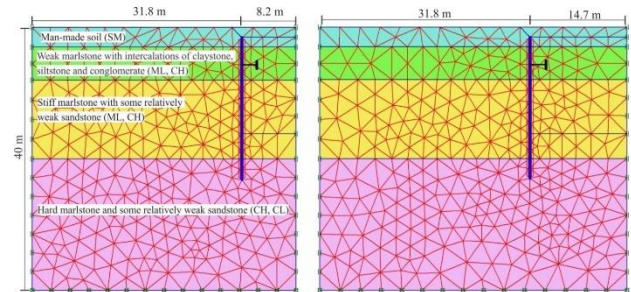


Fig. 8 Finite element mesh in PLAXIS for two different widths of excavation

using the finite element computer program PLAXIS V.8 (PLAXIS BV 2006). For this analysis, a half mesh was used due to geometrical symmetry. A fine mesh size and fourth order 15-node triangular elements were used. A four-layer soil profile was adopted. Fig. 8 shows typical mesh for the excavations where half widths of excavations are 8.2 and 14.7 m. The accuracy of finite element analysis for geotechnical problems depends highly on the selection of the soil model and its individual parameters (Ng *et al.* 2008). The strain hardening (HS) model was chosen for all the soil layers. This model applies a typically non-linear stress-strain relationship for soils (Kulesza *et al.* 2008). Previous studies show that the HS model is suitable for the analysis of deep excavation problems and compared to the Mohr-Coulomb model predicts the ground surface settlements with more accuracy (Ou 2016). In addition to the internal friction angle and cohesion, this model requires eight other input parameters as summarized in Table 1. The reference modulus at 50% of strength (E_{50}^{ref}) and exponential power (m) were determine from results of triaxial tests based on the method described by Surarak *et al.* (2012). As suggested by Brinkgreve (2002), the E_{oed}^{ref} is equal to E_{50}^{ref} and E_{ur}^{ref} is three times of E_{50}^{ref} . The default values of 0.2 and 0.9 were considered for parameters ν_{ur} and R_f , respectively. The input parameters for hardening model were presented in Table 2.

The multiplication of the depth in the unit weight of the soil was considered as the initial vertical stress. The horizontal stress was determined by the multiplication of

Table 1 Input parameters for hardening soil model (Surarak *et al.* 2012)

Parameter	Description	Parameter evaluation
R_f	Failure ratio	$(\sigma_1 - \sigma_3)_f / (\sigma_1 - \sigma_3)_{ur}$
ψ	Dilatancy angle	Function of ε_a and ε_v
E_{50}^{ref}	Reference secant stiffness from drained triaxial test (σ_3/p^{ref})	y-intercept in $\log(\sigma_3/p^{ref}) - \log(E_{50})$ curve
E_{oed}^{ref}	Reference tangent stiffness for oedometer primary loading	y-intercept in $\log(\sigma_1/p^{ref}) - \log(E_{oed})$ curve
E_{ur}^{ref}	Reference unloading/reloading stiffness	y-intercept in $\log(\sigma_3/p^{ref}) - \log(E_{ur})$ curve
m	Exponential power Slope of trend-line in	Slop of trend-line in $\log(\sigma_3/p^{ref}) - \log(E_{50})$ curve
ν_{ur}	Unloading/reloading Poisson's ration	0.20 (default setting)
K_0^{nc}	Coefficient of earth pressure at rest	1-sinf (default setting)

* P^{ref} is reference pressure (100 kN/m² by default setting)

Table 2 Geotechnical properties for the geological layers in the station L2-S17 up to depth 20

Layer –depth	0-3 m	3-8 m	8-20 m	>20 m
Type of geological materials	Coarse-grained man-made soil (SM)	Relatively weak marlstone with intercalations of claystone, siltstone and conglomerate (ML, CH)	Stiff marlstone with some relatively weak sandstone (ML, CH)	Hard marlstone with some relatively weak sandstone
γ_d (kN/m ³)	16.5~17.5	17.0~18.0	17.5~18.5	18.0~19.0
K (cm/s)	$10^{-5} \sim 10^{-4}$	$10^{-6} \sim 10^{-5}$	$10^{-7} \sim 10^{-6}$	$10^{-8} \sim 10^{-7}$
E_{50}^{ref} (MPa)	7	18	22	31
E_{oed}^{ref} (MPa)	7	18	22	31
E_{ur}^{ref} (MPa)	21	54	66	93
C_{uu} (kPa)	20-30	30-50	50-100	100-120
C_{cu} (kPa)	10-20	30-40	30-50	50-70
ϕ_{uu}	14-16	16-18	18-20	20-22
ϕ_{cu}	26-28	24-26	26-28	28-30
K_0	0.54	0.57	0.54	0.51
m	1	0.6	0.7	0.8
ν_{ur}	0.2	0.2	0.2	0.2
R_f	0.9	0.9	0.9	0.9

Table 3 Diaphragm wall properties

Parameters	Wall type		
	Flexible	Medium	Stiff
Bending stiffness EI (kNm ² /m)	5.04×10^4	5.04×10^5	5.04×10^6
Normal stiffness EA (kN/m)	3.427×10^6	3.427×10^7	3.427×10^8
Poisson's ratio	0.15	0.15	0.15
D (m)	0.42	0.42	0.42
W (kN/m/m)	10	10	10

Table 4 Typical construction sequences of station L2-S17

Stage	Construction details
1	Excavate to the top of wall (1.5 m below ground surface)
2	Install the wall
3	Excavate to below the strut level (8 m below the ground surface)
4	Install the strut system
5	Excavate to 17 m below the ground surface

the effective vertical stress in the coefficient of the at-rest lateral earth pressure, $K_0 = 1 - \sin\phi$ (Jaky 1944).

The excavation was retained by the concrete diaphragm wall that is 23 m deep. The wall was propped by one row of struts and the horizontal spacing of struts was about 5 m in average, as shown in Fig. 3(c) (Imansazan Consulting Engineers 2017). The wall is simulated using the elastic plate element. The elastic behavior is defined by the following parameters:

EA, normal stiffness

EI: bending stiffness

ν : Poisson's ratio

Table 3 presents input parameters of diaphragm walls used in the analyses. In this study, three different values for wall stiffness were considered, as presented in Table 3. Based on the approach adopted by Finno *et al.* (2002) and used by Goh *et al.* (2018), a value of 0.42 m was set for the wall thickness (D) so that the area A and moment of inertia I were kept constant, and only the wall elastic modulus E was changed. The steel strut is modelled by means of a fixed-end anchor for which the normal stiffness, EA, is a required input parameter. The strut is placed horizontally at a spacing of 5 meters with an EA value of 2×10^6 kN. The interface between the wall and the soil is modeled at both sides by means of interfaces. The interfaces allow for the specification of a reduced wall friction compared to the friction in the soil. As proposed by Likitlersuang *et al.* (2013) and Schweiger *et al.* (2009), the strength reduction factor of interface element, R_{inter} , was considered as 0.7.

For the boundary conditions, rollers were selected at the side boundaries to allow vertical displacements and pinned was applied at the base to prevent any displacements. The station was excavated to the maximum depth of 17 m with five stages of excavation (Table 4). As proposed by Hsieh and Ou (1998), the width of the model should be typically two times larger than the excavation depth to remove the effect of the boundary restraints on the ground displacements. The original groundwater table was assumed to be 8 m below the ground surface in the retained soil. Then, the groundwater table was progressively lowered with excavation during each phase.

Simulated lateral wall deflections and ground surface settlements are presented in the next section.

5. Results

Effects of wall stiffness on deformation induced by the excavation of station L2-S17 were investigated for widths of 8.2 and 14.7 m. The important results are as follow:

a) *Effect of wall stiffness on deformation induced by the excavation with a width of 8.2 m*

Fig. 9(a)-(c) shows a comparison of wall deflection profiles at various stages of construction for three different values of wall stiffness. The wall deflection increases with increasing excavation depth. This increasing can be attributed to passive and active lateral pressure. Zahmatkesh and Choobbasti (2015) believe that the active pressure increases and passive pressure decreases with increase of excavation depth. Hence, as shown in Fig. 9, at the last stage of excavation, deflection wall is more significant. At

an excavation depth of 8 m and before (stage 3) and after (stage 4) installation of strut, the wall lateral displacement is in cantilever mode, i.e., the lateral displacement is larger at the top of the wall. This mode of deformation relies on the passive soil resistance for its stability (Zahmatkesh and Choobbasti 2015). In agreement with previous study by Goh *et al.* (2018), the installation of strut results in lateral restraint of the wall movement above the level of the installed strut. As excavation reaches to the final depth (stage 5), the wall shows the braced excavation mode with a bulge in the third layer of the soil profile.

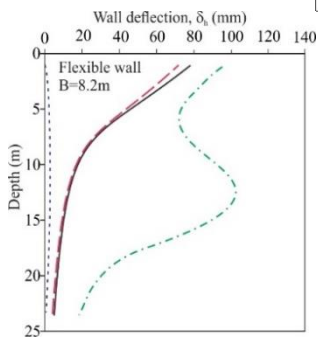
The comparison of wall deflection profiles for three different values of wall stiffness reveals a general trend that the wall displacements decrease with increasing wall stiffness. The maximum wall deflections (δ_{hm}) in the last excavation stage for flexible, medium and stiff walls are 102.3, 69.4 and 44.3 mm, respectively, which relatively occur at the medium part of the walls. Previous studies (e.g., Goh *et al.* 2018, Masuda *et al.* 1994, Zahmatkesh and Choobbasti 2015) showed that the wall stiffness have a significant influence on the magnitude of wall deflection. Generally, the results show that the wall stiffness only affects the magnitude of wall deflection rather than the shape of wall deflection profile. A ten unit increase in the bending stiffness (EI) results in a 1.5 unit reduction in the δ_{hm} . The ratio of δ_{hm} to excavation depth (H_e) for flexible, medium and stiff wall is 0.60, 0.41 and 0.26%, which is relatively consistent with Bentler (1998) and Wang *et al.* (2012) findings.

Fig. 10(a)-10(c) shows total displacements at the final stage for three different values of wall stiffness. Fig. 11(a)-(c) also shows the simulated ground surface settlements for three different values of wall stiffness. In agreement with previous research by Ou and Hsieh (2011), the mode of deformation is relatively similar for all three values of wall stiffness. In all three cases, the ground settlements progressively increase with each construction stage, especially following stage 5. As evident from this figure, the ground settlements decrease and the maximum ground settlement (δ_{vm}) occurs at the larger distance from the wall with increasing wall stiffness. The δ_{vm} value at the end of excavation for flexible, medium and stiff walls is 70.8, 50.0 and 36.9 mm, and occurs at 5.5, 8.2 and 16.5 m from the wall, respectively. In fact, a ten unit increase in bending stiffness of the wall results in a 1.5 unit reduction in the δ_{vm} . Investigation of many historical excavations by Bentler (1998) shows that the ratio between δ_{vm} and δ_{hm} mostly varies between 0.5 and 1. This study indicates that the ratio of δ_{vm}/δ_{hm} approaches to 1 with increasing wall stiffness.

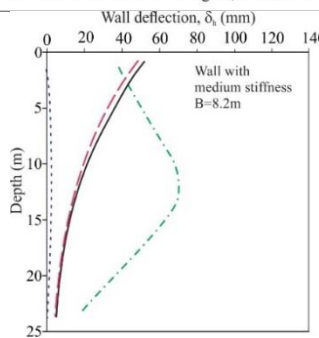
Hsieh and Ou (1998) based on the analysis of 9 case histories presented a concave settlement profile for the bulging mode of lateral wall deformations. In this mode, the maximum settlement is assumed to occur at 0.5 H_e . They showed the settlement at the wall face and at 2 H_e from the wall is approximated to 50% and 10% of the maximum settlement and at 4 H_e from the wall is negligible. Fig. 12 shows that the surface settlements at the last stage of excavation are larger than those predicted by using Hsieh and Ou (1998) method.

b) *Effect of wall stiffness on deformation induced by the excavation with a width of 14.7 m*

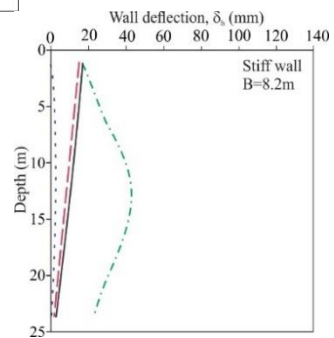
Stage 2, after wall installation - - - Stage 4, after installation of struts —
 Stage 3, before installation of struts - - - Stage 5, at the end of excavation - - -



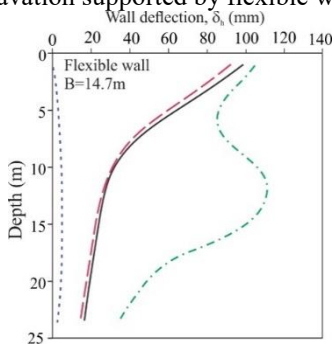
(a) Wall deflection for the narrower excavation supported by flexible wall



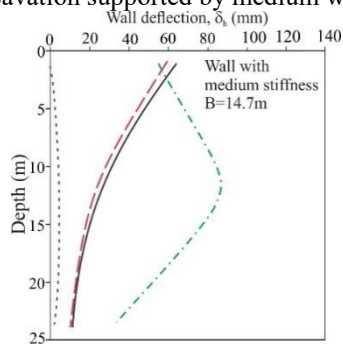
(b) Wall deflection for the narrower excavation supported by medium wall



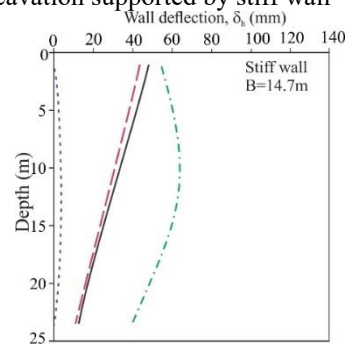
(c) Wall deflection for the narrower excavation supported by stiff wall



(d) Wall deflection for the wider excavation supported by flexible wall

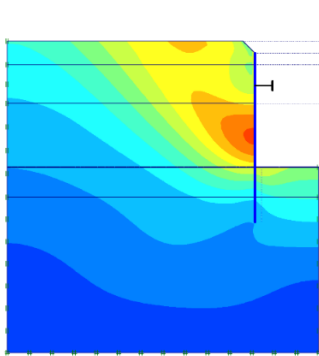


(e) Wall deflection for the wider excavation supported by medium wall

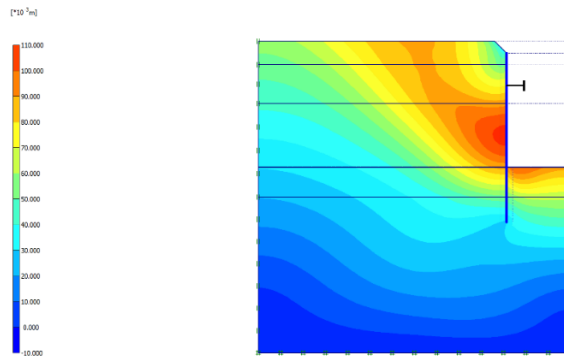


(f) Wall deflection for the wider excavation supported by stiff wall

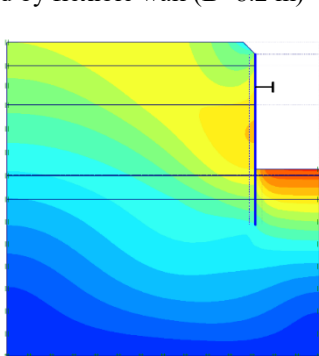
Fig. 9 Predicted lateral wall deflections at various stages of excavation. The width of excavation (B) is presented in each photo



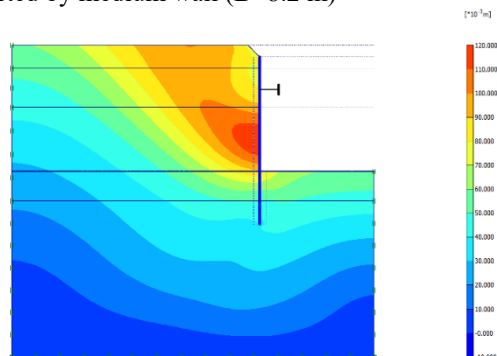
(a) Total displacements for the narrower excavation supported by flexible wall (B=8.2 m)



(b) Total displacements for the narrower excavation supported by medium wall (B=8.2 m)

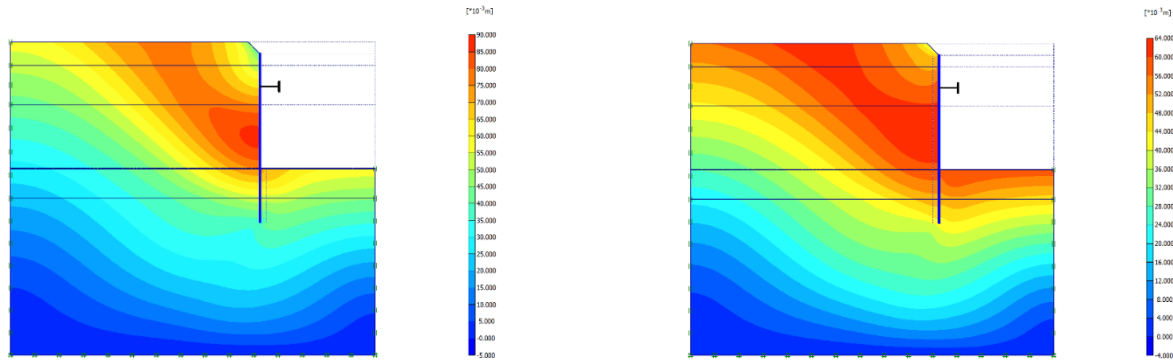


(c) Total displacements for the narrower excavation supported by stiff wall (B=8.2 m)



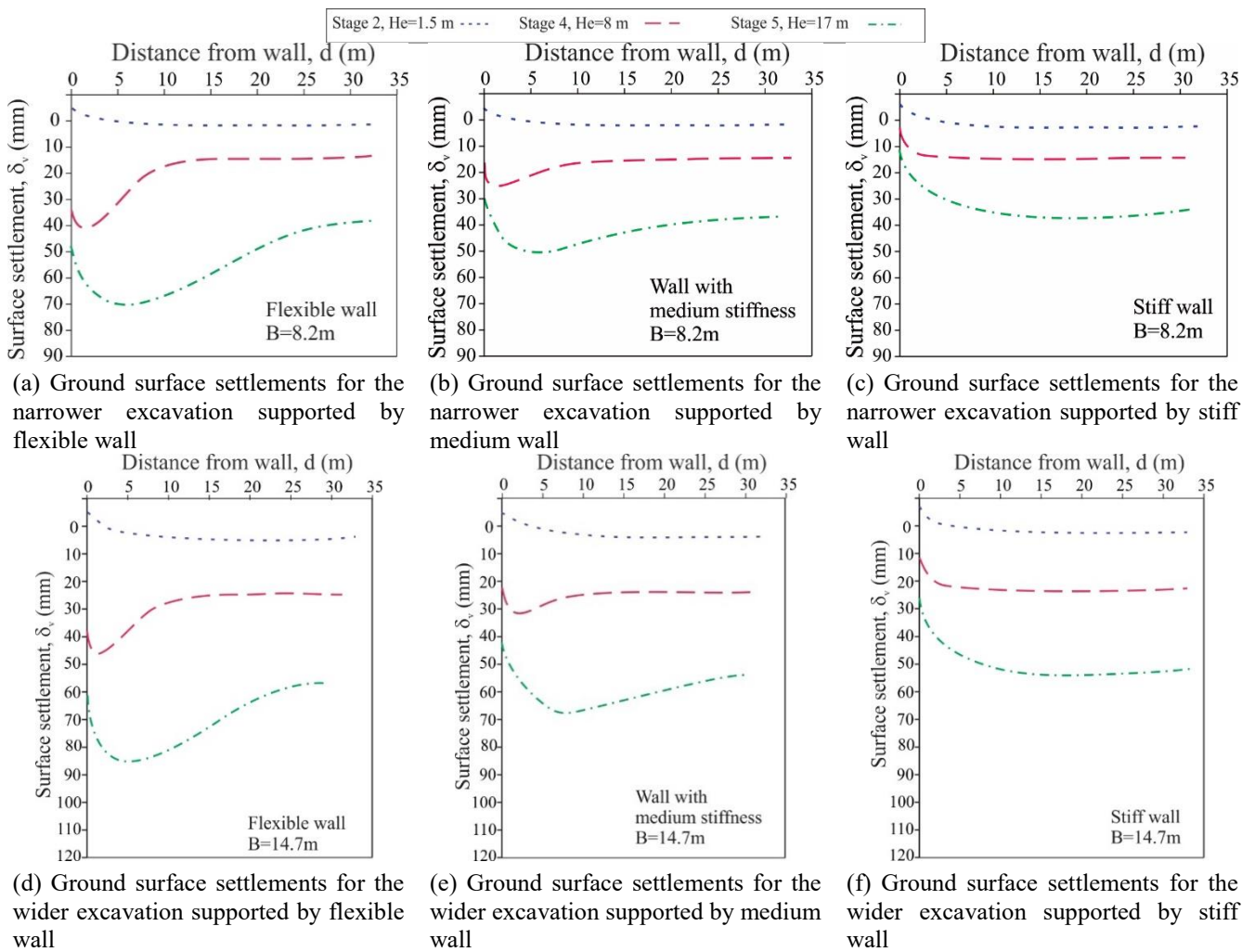
(d) Total displacements for the wider excavation supported by stiff wall (B=14.7 m)

Fig. 10 Total displacements at the final stage of excavation



(e) Total displacements for the wider excavation supported by medium wall (B=14.7 m) (f) Total displacements for the wider excavation supported by stiff wall (B=14.7 m)

Fig. 10 Continued



(a) Ground surface settlements for the narrower excavation supported by flexible wall (b) Ground surface settlements for the narrower excavation supported by medium wall (c) Ground surface settlements for the narrower excavation supported by stiff wall (d) Ground surface settlements for the wider excavation supported by flexible wall (e) Ground surface settlements for the wider excavation supported by medium wall (f) Ground surface settlements for the wider excavation supported by stiff wall

Fig. 11 Predicted surface settlements at various stages of excavation. The width of excavation (B) is presented in each photo

Fig. 9(d)-9(f) shows a comparison of wall deflection profiles at various stages of construction for the wider excavation. The shape of wall deflection profiles are similar to those obtained for the narrower excavations. However, the magnitude of displacements is larger here. In this condition, the δ_{hm} in the last excavation stage for flexible, medium and stiff walls is 116.6, 86.0 and 62.5 mm, respectively. It can be said that a ten unit increase in

bending stiffness of the wall results in a 1.4 unit decrease in the δ_{hm} . The ratio of δ_{vm}/He is 0.68, 0.51 and 0.36%, respectively, for the excavations supported by flexible, medium and stiff walls.

Fig. 10(d)-9(f) shows total displacements at the final stage for three different values of wall stiffness. Fig. 11(d)-9(f) also shows the simulated ground surface settlement for the wider excavation. The shapes of ground settlement are

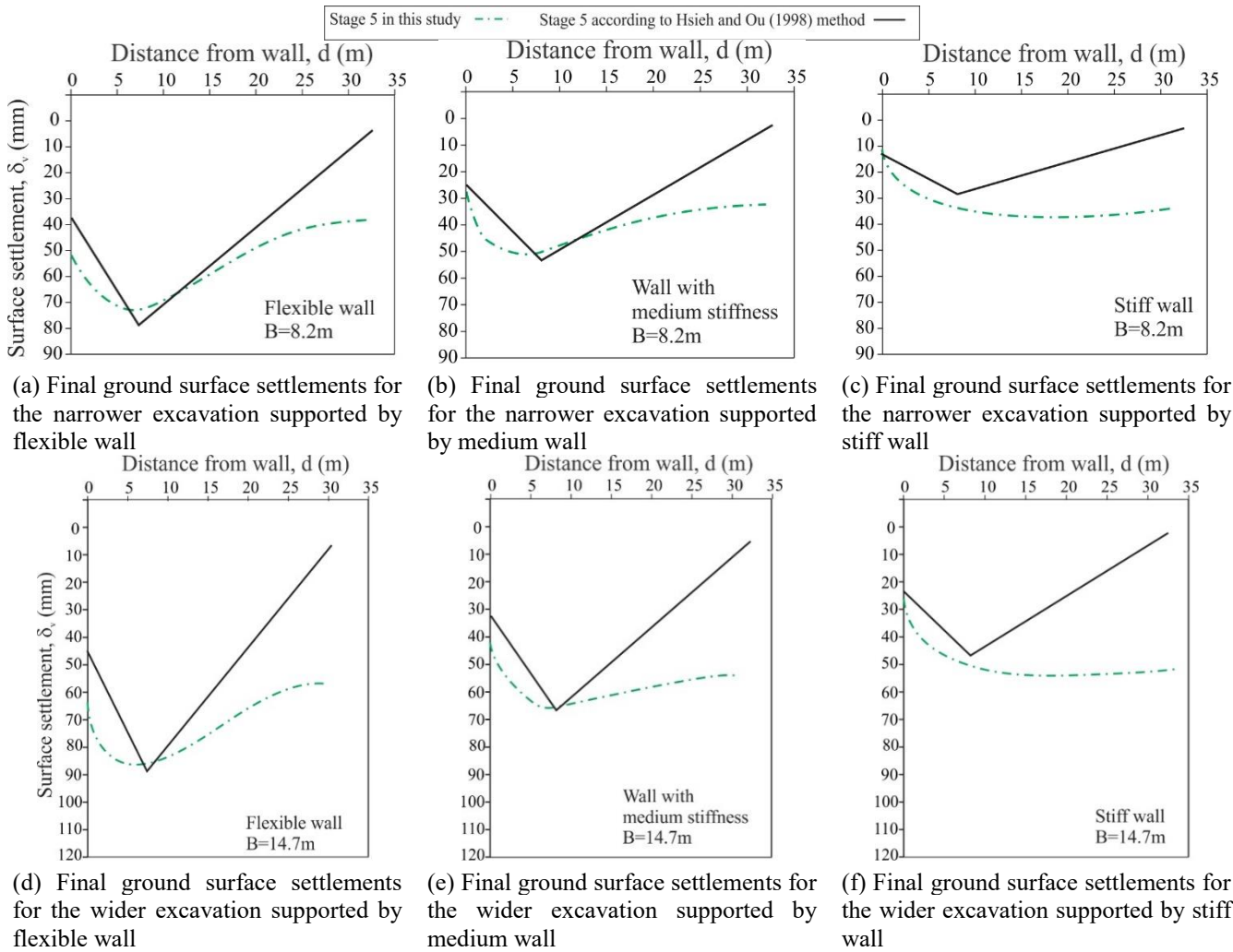


Fig. 12 Comparison of surface settlements predicted for stage 5 in this study with those predicted by Hsieh and Ou (1998) method. The width of excavation (B) is presented in each graph

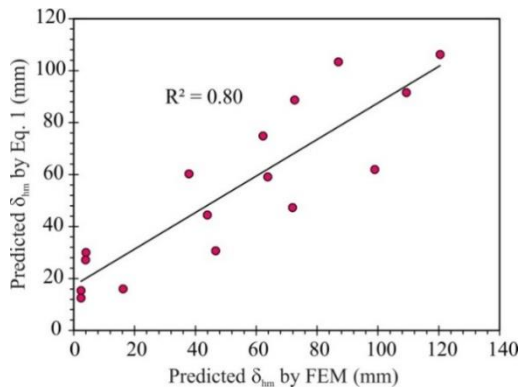


Fig. 13 Comparison of δ_{hm} calculated by Eq. (1) and δ_{hm} predicted by FEM

similar to those obtained from the narrower excavations; however, as evident from these figures, the ground settlement increases with increasing the width of excavation. The values of δ_{vm} for the excavations supported by flexible, medium and stiff walls are 85.7, 66.7 and 56.5 mm, respectively. The maximum of settlement occurred at the larger distance from the wall compared to the narrower excavations. It is at 6.1, 9.1 and 24.2 m from the wall,

Table 5 Summarization of analyses

B (m)	He (m)	EI (kNm ² /m)	δ_{hm} (mm)	δ_{vm} (mm)
8.2	1.5	50400	2.5	1.8
	8	50400	81.8	33.2
	17	50400	102.3	70.8
	1.5	504000	2.5	1.9
	8	504000	54.2	19.3
	17	504000	69.4	50.0
14.7	1.5	5040000	2.4	1.8
	8	5040000	33.8	14.8
	17	5040000	44.3	36.9
	1.5	50400	4.1	4.8
	8	50400	106.7	39.5
	17	50400	116.6	85.7
	1.5	504000	4.1	4.8
	8	504000	60.9	25.8
	17	504000	86.0	66.7
	1.5	5040000	4.1	3.7
	8	5040000	44.2	25.3

Table 5 Continued

B (m)	He (m)	EI (kNm ² /m)	δ_{hm} (mm)	δ_{vm} (mm)
14.7	17	5040000	62.5	56.5

respectively, for the flexible, medium and stiff walls.

6. Discussion

This study performed a series of 2D finite element analyses to investigate the effect of wall stiffness and excavation width on deformation-induced by excavation.

Table 5 indicates the calculated values of δ_{hm} and δ_{vm} for different values of excavation width (B), excavation depth (He) and bending stiffness of the wall (EI). As seen, the wall deflection and ground surface settlement increase with increasing excavation depth and width. The stiffness of the wall has no serious effect on the shape of wall horizontal deflection and ground surface settlement. The change in maximum wall deflection and ground settlement with considerable increase in wall stiff system is marginal, so the lower wall stiffness produces the larger displacements at the wall.

Most previous studies (e.g., Hsieh *et al.* 2003, Hsiung and Dao 2015, Ng *et al.* 2004, Yeow *et al.* 2006) show that the FEM can predict the wall deflection with good accuracy. If the predicted wall deflections are near the actual values, the following relationship can be presented to evaluate the effect of wall stiffness and excavation depth and width on the maximum wall deflection

$$\delta_{hm} = 2.3B + 4.9He - 0.0062EI - 10 \quad (1)$$

where δ_{hm} is the maximum wall deflection in mm, B is the excavation width in m, He is the excavation depth in m and EI is the wall bending stiffness in Nm²/m. Fig. 13 displays the δ_{hm} estimated using Eq. (1) versus the δ_{hm} predicted by FEM. The determination coefficient of model (R^2) reveals that 80% of variations occurring in the δ_{hm} are controlled by the model independent variables.

The ground settlements predicted by the FEM were larger than those predicted by the empirical method of Hsieh and Ou (1998). Previous studies (e.g., Hsieh *et al.* 2003, Hsiung and Dao 2015, Ng *et al.* 2004, Yeow *et al.* 2006) also show that the FEM usually gives better predictions for wall deflection than for ground settlement. Of course, it should be noted that the wall stiffness was not considered in the most of the empirical methods. This study shows that settlement influence zones for excavations in marly layers can be affected by the wall stiffness. For excavation supported by the flexible walls, the ground settlement distribution was more or less similar to that predicted by the empirical methods (Fig. 12(a), 12(d)). The settlement influence zones for excavations supported by the wall with higher stiffness are different from those predicted by Hsieh and Ou (1998) method (Fig. 12(b)-12(c), 12(e)-12(f)) and are similar to those presented by Hung *et al.* (2014). The analyses show that settlements decrease by increasing the wall stiffness, also the settlement influence zone becomes wider and the δ_{vm} occurs at a larger distance

from the wall.

According to field observations, large wall displacements and ground surface settlements (more than 100 mm) occur when the excavation are retained with the flexible wall. Given that the station L2-S17 is located in the densely populated area, this large deformation may influence the safety of adjacent buildings. Therefore, it is suggested that the stiff walls are used for supporting the deep excavations in the marly layers.

7. Conclusions

This paper investigates the effect of wall stiffness and deep excavation width on the diaphragm wall displacements and ground surface settlements in marly layers. An underground station excavation of the Tabriz Metro Line 2 project (station L2-S17) was used as a case study. The geological investigations showed that the subsurface layers in the station were mostly composed of weak to hard marlstone with some interlayers of siltstone and claystone. The UCS values of samples (most of them having the UCS lower than 500 kPa) and the ductile behavior of them during uniaxial, triaxial and direct shear tests suggest that the marlstones in this station behave more like hard soil than rock. Two dimension modelling and analyses by finite element method showed the following results:

- The wall deflections and ground settlements increase with increasing excavation depth and width.
- The wall stiffness only affects the magnitude of wall deflections and ground settlements rather than the shape of deformations.
- The maximum final wall deflection and ground settlement for the narrower excavation (B=8.2 m) supported by the flexible wall were 102.3 and 70.8 mm, respectively. A 10 unit increase in the wall stiffness approximately led to 30-40% reduction of the δ_{hm} and δ_{vm} for the narrower excavations and 20-30% reduction of them for the wider excavations.
- The analyses suggest that the settlement influence zones become wider and the δ_{vm} occurs at a larger distance from the wall with increasing the wall stiffness.

References

- Ahmed, S.M. and Fayed, A.L. (2015), "Mitigation of risks associated with deep excavations: State of the art review", *Proceedings of the Industry Academia Collaboration Conference (IAC 2015)*, Cairo, Egypt, April.
- Ashgari Kaljahi, E. Barzegari, G. and Jalali-Milani, S. (2019), "Assessment of the swelling potential of Baghmisheh marls in Tabriz, Iran", *Geomech. Eng.*, **18**(3), 267-275. <http://doi.org/10.12989/gae.2019.18.3.267>.
- Ashgari-Kaljahi, E., Yousefi-Bavil, K. and Babazadeh, M. (2015), "A study of ground natural temperature along Tabriz metro line 2, Iran", *Eng. Geol. Soc. Territory*, **6**, 295-298. https://doi.org/10.1007/978-3-319-09060-3_49.
- Barzegari, G., Shayan, F. and Chakeri, H. (2018), "Investigations on Geotechnical Aspects for TBM Specification on the Tabriz Metro Line 3, Iran", *Geotech. Geol. Eng.*, **36**(6), 3639-3663. <http://doi.org/10.1007/s10706-018-0563-2>.
- Bentler, D.J. (1998), "Finite element analysis of deep

- excavations”, Ph.D. Dissertation, Virginia Polytechnic Institute and State University, Blacksburg, Virginia. U.S.A.
- Brinkgreve, R.B.L. (2002), *Plaxis 2D-Version 8 Manuals*, A.A.Balkema, The Netherlands.
- Cheshomi, A. and Ghodrati, M. (2015), “Estimating Menard pressuremeter modulus and limit pressure from SPT in silty sand and silty clay soils. A case study in Mashhad, Iran”, *Geomech. Geoeng.*, **10**(3), 194-202. <https://doi.org/10.1080/17486025.2014.933894>.
- Do, N.A. Dias, D., Oreste, P. and Djeran-Maigre, I. (2014), “2D numerical investigations of twin tunnel interaction”, *Geomech. Eng.*, **6**(3), 263-275. <http://dx.doi.org/10.12989/gae.2014.6.3.000>.
- Dobereiner, L. (1984), “Engineering geology of weak sandstones”, Ph.D. Dissertation, University of London, London, U.K.
- Dong, Y., Burd, H., Houlby, G. and Hou, Y. (2014), “Advanced finite element analysis of a complex deep excavation case history in Shanghai”, *Front. Struct. Civ. Eng.*, **8**(1), 93-100. <https://doi.org/10.1007/s11709-014-0232-3>.
- Edalat, K., Vahdatirad, M.J., Ghodrati, H., Firouzian, S. and Barari, A. (2010), “Choosing TBM for Tabriz subway using multi criteria method”, *J. Civ. Eng. Manag.*, **16**(4), 531-539. <https://doi.org/10.3846/jcem.2010.59>.
- Finno, R.J. Bryson, S. and Calvello, M. (2002), “Performance of a stiff support system in soft clay”, *J. Geotech. Geoenviron. Eng.*, **128**(8), 660-671. [https://doi.org/10.1061/\(ASCE\)1090-0241\(2002\)128:8\(660\)](https://doi.org/10.1061/(ASCE)1090-0241(2002)128:8(660)).
- Firuzi, M. Asghari-Kaljahi, E. and Akgün, H. (2019), “Correlations of SPT, CPT and pressuremeter test data in alluvial soils. Case study: Tabriz Metro Line 2, Iran”, *Bull. Eng. Geol. Environ.*, 1-20. <https://doi.org/10.1007/s10064-018-01456-0>.
- Fonte, J.B. (2010), “Numerical modeling of excavations below the water table”, Ph.D. Dissertation, Universidad Do Porto, Porto, Portugal.
- Georgiannou, V., Burland, J. and Hight, D. (1990), “The undrained behaviour of clayey sands in triaxial compression and extension”, *Geotechnique*, **40**(3), 431-449. <https://doi.org/10.1680/geot.1990.40.3.431>.
- Ghahreman, B. (2004), “Analysis of ground and building response around deep excavations in sand”, Ph.D. Dissertation, University of Illinois at Urbana-Champaign, Champaign Illinois, U.S.A.
- Ghazvinian, A., Fathi, A. and Moradian, Z. (2008), “Failure behavior of marlstone under triaxial compression”, *Int. J. Rock Mech. Min. Sci.*, **5**(45), 807-814. <https://doi.org/10.1016/j.ijrmm.2007.09.006>.
- Goh, A., Fan, Z., Hanlong, L., Wengang, Z. and Dong, Z. (2018), “Numerical Analysis on Strut Responses Due to One-Strut Failure for Braced Excavation in Clays”, *Proceedings of the 2nd International Symposium on Asia Urban GeoEngineering*, Changsha, China, November.
- He, M. (2014), “Latest progress of soft rock mechanics and engineering in China”, *J. Rock Mech. Geotech. Eng.*, **6**(3), 165-179. <https://doi.org/10.1016/j.jrmge.2014.04.005>.
- Hesami, S., Ahmadi, S., Ghalesari, A.T. and Hasanzadeh, A. (2013), “Ground surface settlement prediction in urban areas due to tunnel excavation by the NATM”, *Elec. J. Geotech. Eng.*, **18**, 1961-1972.
- Hooshmand, A. Aminfar, M.H. Asghari, E. and Ahmadi, H. (2012), “Mechanical and physical characterization of Tabriz marls, Iran”, *Geotech. Geol. Eng.*, **30**(1), 219-232.
- Hsieh, P., Kung, T., Ou, C. and Tang, Y. (2003), “Deep excavation analysis with consideration of small strain modulus and its degradation behavior of clay”, *Proceedings of the 12th Asian Regional Conference on Soil Mechanics and Geotechnical Engineering*, Singapore, August.
- Hsieh, P.G. and Ou, C.Y. (1998), “Shape of ground surface settlement profiles caused by excavation”, *Can. Geotech. J.*, **35**(6), 1004-1017. <https://doi.org/10.1139/t98-056>.
- Hsiung, B.C.B. and Dao, S.D. (2015), “Prediction of ground surface settlements caused by deep excavations in sands”, *Geotech. Eng.*, **46**(3), 111-118. <https://doi.org/10.1007/s10706-011-9464-3>.
- Hung, C. Ling, H.I. and Kaliakin, V.N. (2014), “Finite element simulation of deep excavation failures”, *Transport. Infrastruct. Geotechnol.*, **1**(3-4), 326-345. <https://doi.org/10.1007/s40515-014-0011-6>.
- Imansazan Consulting Engineers (2017), “Conceptual design of eastern stations of TML2 project”, Presented to TURO.
- ISRM (1981), *Rock Characterization Testing and Monitoring*, Pergamon Press, New York, U.S.A.
- Jaky, J. (1944), “The coefficient of earth pressure at rest”, *J. Soc. Hung. Arch. Eng.*, 355-358.
- Jalali-Milani, S. Asghari-Kaljahi, E., Barzegari, G. and Hajialilue-Bonab, M. (2017), “Consolidation deformation of Baghmisheh marls of Tabriz, Iran”, *Geomech. Eng.*, **12**(4), 561-577. <http://doi.org/10.12989/gae.2017.12.4.561>.
- Kanji, M.A. (2014), “Critical issues in soft rocks”, *J. Rock Mech. Geotech. Eng.*, **6**(3), 186-195. <https://doi.org/10.1016/j.jrmge.2014.04.002>.
- Kulesza, R. Boussoulas, N. and Marr, W.A. (2008), “Deep excavations in hard sandy clays for stations and shafts of the Athens Metro Stavros extension”, *Proceedings of the 6th International Conference on Case Histories in Geotechnical Engineering*, Rolla, Missouri, U.S.A., August.
- Likitlersuang, S., Surarak, C., Wanatowski, D., Oh, E. and Balasubramaniam, A. (2013), “Finite element analysis of a deep excavation: A case study from the Bangkok MRT”, *Soils Found.*, **53**, 756-773. <http://dx.doi.org/10.1016/j.sandf.2013.08.013>.
- Masuda, T. Einstein, H.H. and Mitachi, T. (1994), “Prediction of lateral deflection of diaphragm wall in deep excavations”, *Doboku Gakkai Ronbunshu*, **505**, 19-29.
- Mohammadi, S. Firuzi, M. and Asghari Kaljahi, E. (2015), “Geological-geotechnical risk in the use of EPB-TBM, case study: Tabriz Metro, Iran”, *Bull. Eng. Geol. Environ.*, **75**(4), 1571-1583. <https://doi.org/10.1007/s10064-015-0797-7>.
- Nabavi, M. (1976), *An Introduction to the Geology of Iran*, in *Geological Survey of Iran* (in Persian).
- Nawel, B. and Salah, M. (2015), “Numerical modeling of two parallel tunnels interaction using three-dimensional finite elements method”, *Geomech. Eng.*, **9**(6), 775-791. <https://doi.org/10.12989/gae.2015.9.6.775>.
- Ng, C.W., Huang, H. and Liu, G. (2008), “Geotechnical Aspects of Underground Construction in Soft Ground”, *Proceedings of the 6th International Symposium (IS-Shanghai 2008)*, Shanghai, China, April.
- Ng, C.W., Leung, E.H. and Lau, C. (2004), “Inherent anisotropic stiffness of weathered geomaterial and its influence on ground deformations around deep excavations”, *Can. Geotech. J.*, **41**(1), 12-24. <https://doi.org/10.1139/t03-066>.
- Nikvar Hassani, A. Katibeh, H. and Farhadian, H. (2015), “Numerical analysis of steady-state groundwater inflow into Tabriz line 2 metro tunnel, northwestern Iran, with special consideration of model dimensions”, *Bull. Eng. Geol. Environ.*, **75**(4), 1617-1627. <http://dx.doi.org/10.1007/s10064-015-0802-1>.
- Ou, C.Y. (2016), “Finite element analysis of deep excavation problems”, *J. Geoeng.*, **11**(1), 1-12. [http://dx.doi.org/10.6310/jog.2016.11\(1\).1](http://dx.doi.org/10.6310/jog.2016.11(1).1).
- Ou, C.Y. and Hsieh, P.G. (2011), “A simplified method for predicting ground settlement profiles induced by excavation in soft clay”, *Comput. Geotech.*, **38**(8), 987-997.

- <https://doi.org/10.1016/j.compgeo.2011.06.008>.
- P.O. Rahvar Consulting Engineers (2008), "Geotechnical investigation report of TML2 project", Presented to TURO.
- Sabzi, Z. and Fagher, A. (2015), "The performance of buildings adjacent to excavation supported by inclined struts", *Int. J. Civ. Eng.*, **13**(1), 1-13.
- Schweiger, H. Scharinger, F. and Lüftenegger, R. (2009), "3D finite element analysis of a deep excavation and comparison with in situ measurements", *Geotech. Aspects Undergr. Construct. Soft Ground*, 193-199.
- Surarak, C., Likitlersuang, S., Wanatowski, D., Balasubramaniam, A., Oh, E. and Guan, H. (2012), "Stiffness and strength parameters for hardening soil model of soft and stiff Bangkok clays", *Soils Found.*, **52**(4), 682-697. <https://doi.org/10.1016/j.sandf.2012.07.009>.
- Tenando, E. (2004), "Strength properties and mineralogy of Singapore old alluvium", M.Sc. Thesis, National University of Singapore, Singapore.
- Wang, P.X., Cui, T., Shi, J.S. and Dai, R.P. (2012), "Analysis and treatment of diaphragm wall intrusion-clearance of Metro Station in soft ground", *Adv. Mater. Res.*, **374**, 2232-2238. <https://doi.org/10.4028/www.scientific.net/AMR.374-377.2232>.
- Yeow, H., Nicholson, D. and Simpson, B. (2006), "Comparison and feasibility of three dimensional finite element modelling of deep excavations using non-linear soil models", *Proceedings of the International Conference on Numerical Simulation of Construction Processes in Geotechnical Engineering for Urban Environment*, Bochum, Germany, March.
- Zahmatkesh, A. and Choobbasti, A. (2015), "Evaluation of wall deflections and ground surface settlements in deep excavations", *Arab. J. Geosci.*, **8**(5), 3055-3063. <https://doi.org/10.1007/s12517-014-1419-6>.
- Zheng, G., Du, Y., Cheng, X., Diao, Y., Deng, X. and Wang, F. (2017), "Characteristics and prediction methods for tunnel deformations induced by excavations", *Geomech. Eng.*, **12**(3), 361-397. <https://doi.org/10.12989/gae.2017.12.3.361>.